

Effects of temperature on the surface plasmon resonance at a metal–semiconductor interface

H.P. Chiang^{a,b,*}, C.-W. Chen^a, J.J. Wu^a, H.L. Li^a, T.Y. Lin^a, E.J. Sánchez^c, P.T. Leung^{c,*}

^a Institute of Optoelectronic Sciences, National Taiwan Ocean University, Keelung, Taiwan, ROC

^b Institute of Physics, Academia Sinica, Taipei, Taiwan, ROC

^c Department of Physics, Portland State University, P. O. Box 751, Portland, OR 97207-0751, USA

Received 26 January 2006; received in revised form 8 February 2007; accepted 11 February 2007

Available online 20 February 2007

Abstract

The effects due to elevated temperatures on the surface plasmon (SP) at a metal–semiconductor interface are studied both experimentally and theoretically. In particular, a junction made of silver and amorphous silicon is fabricated and the interfacial plasmon is excited optically via the Kretschmann geometry. Both the reflectance and phase monitoring of the response of the junction have been studied as a function of temperature from 300 K to 380 K. Theoretical simulations have been carried out to understand the observed data, using a previously established model for the temperature-dependent optical constants of the metal, together with empirically fitted data for those of the semiconductor. Reasonable qualitative comparison between experimental data and simulation is obtained. It is found that the strength of the SP at the junction will decrease as temperature increases, and the methodology of the present experiment may provide a way to quantify such a decrease in the operation efficiency of the junction. In addition, it is shown that, by monitoring the resonance angle, such a junction may act as a temperature sensor with sensitivity possibly higher than the previous ones which employed a bare metal film in the Kretschmann geometry.

© 2007 Elsevier B.V. All rights reserved.

Keywords: Surface plasmon resonance; Metal–semiconductor junction; Temperature effects

1. Introduction

It is well known that the Schottky junction, formed by the interface of a semiconductor and a metal, has many applications including those in the field of solar-cell technology [1]. It has also been known for some time, that one approach to enhance the quantum efficiency of such a device is to couple the external light to excite the surface plasmon (SP) at the metal–semiconductor interface of the junction [2,3]. Here SP refers to the collective oscillation of the free electrons at the interface and once excited, it strongly couples to the external light under resonance condition.

When this happens, large photocurrents will be generated and hence larger quantum efficiency will be achieved.

Optical excitation of SPs at flat interfaces was developed in the late 1960s via the attenuated total reflection method [4]. In our present study, we adopt the Kretschmann geometry with a metal–semiconductor (MS) junction coated on a quartz prism (Fig. 1). Note that unlike previous experiments with the Kretschmann geometry [3], we have utilized a semiconductor film coated on the metal, which enables the SP to be excited at the MS interface. Both the intensity and the phase difference between the p and s reflected wave will be monitored as a signature of the excitation of the SP at the junction interface. Our focus here is on the temperature effects on this SP enhanced mechanism for the operation of the junction. Alternatively, our study will also reveal the possibility of employing such a SP-driven device as a temperature sensor with high sensitivity [5,6]. While there have been many previous studies on the temperature effects for the operation of a MS junction [7,8], none of these has been conducted in conjunction with the SP-enhanced mechanism. An interesting aspect in this study is that, as we

* Corresponding authors. Chiang is to be contacted at Institute of Optoelectronic Sciences, National Taiwan Ocean University, Keelung, Taiwan, ROC. Leung, Department of Physics, Portland State University, P. O. Box 751, Portland, OR 97207-0751, USA. Tel.: +886 2 24622192 6702; fax: +886 2 24634360.

E-mail addresses: hpchiang@mail.ntou.edu.tw (H.P. Chiang), hopl@pdx.edu (P.T. Leung).

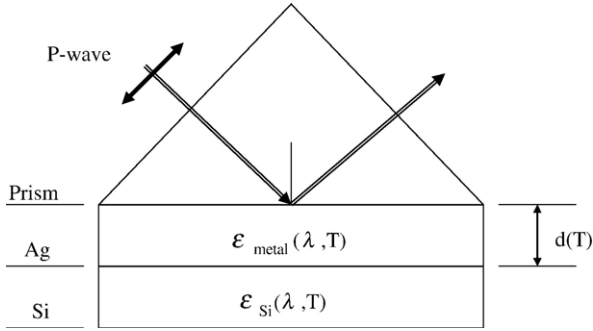


Fig. 1. Configuration of SPR-driven MS junction.

shall see, while the quantum efficiency of a MS junction is expected to increase with temperature in case the barrier height decreases as temperature rises [7,8], the SP mechanism also decreases in its enhancement due to the large damping the free electrons undergo at high temperatures.

Hence we have in this case two competing mechanisms which determine the final operational efficiency of a SP-enhanced MS junction at elevated temperatures. Since the temperature variation of the barrier height has been studied intensively in the literature [7,8], it will be of interest to investigate the temperature effects when the SP mechanism is applied to enhance the operation of such a junction.

2. Experimental section

The experimental setup is shown in Fig. 2 [9]. Two He–Ne lasers of wavelengths 632.8 nm and 1.15 μm, respectively, have

been employed in our system to study the wavelength dependence in phase and reflectivity measurement. Linearly polarized light with angular frequency ω_0 from a He–Ne laser is introduced through a polarizer. The light is then directed into an electro-optic modulator (ConOptics) with a fast axis in the horizontal direction, the light is then reflected from a quartz prism ($n_p = 1.452$) coated with a thin MS film which is in contact with a temperature controller. The film is coated by using an electron beam evaporator and annealed to optimize film uniformity. The laser light then passes through an analyzer AN_t . Both the transmission axes of the polarizer and analyzer are at 45° relative to the horizontal polarization direction. The light is then detected by a photodetector which generates an electric signal and is phase-locked by a lock-in amplifier. A sawtooth signal with angular frequency ω and half-wave voltage $V_{\lambda/2}$ is applied to the electro-optic modulator. From Jones' calculus, the electric field arriving at the photodetector can be described by

$$E_t = \frac{1}{2\sqrt{2}} \left[|r_p| e^{i(\frac{\omega t}{2} + \phi_p)} + |r_s| e^{i(\frac{-\omega t}{2} + \phi_s)} \right] \begin{bmatrix} 1 \\ 1 \end{bmatrix} e^{i\omega_0 t}, \quad (1)$$

and therefore the corresponding detected intensity is

$$I_t = \frac{1}{4} \left[\frac{|r_p|^2 + |r_s|^2}{2} + |r_p| |r_s| \cos(\omega t + \phi_p - \phi_s) \right], \quad (2)$$

where r_p , r_s , ϕ_p , ϕ_s are the field reflectivity and phases of the p-wave and s-wave, respectively. Since only the p-wave can

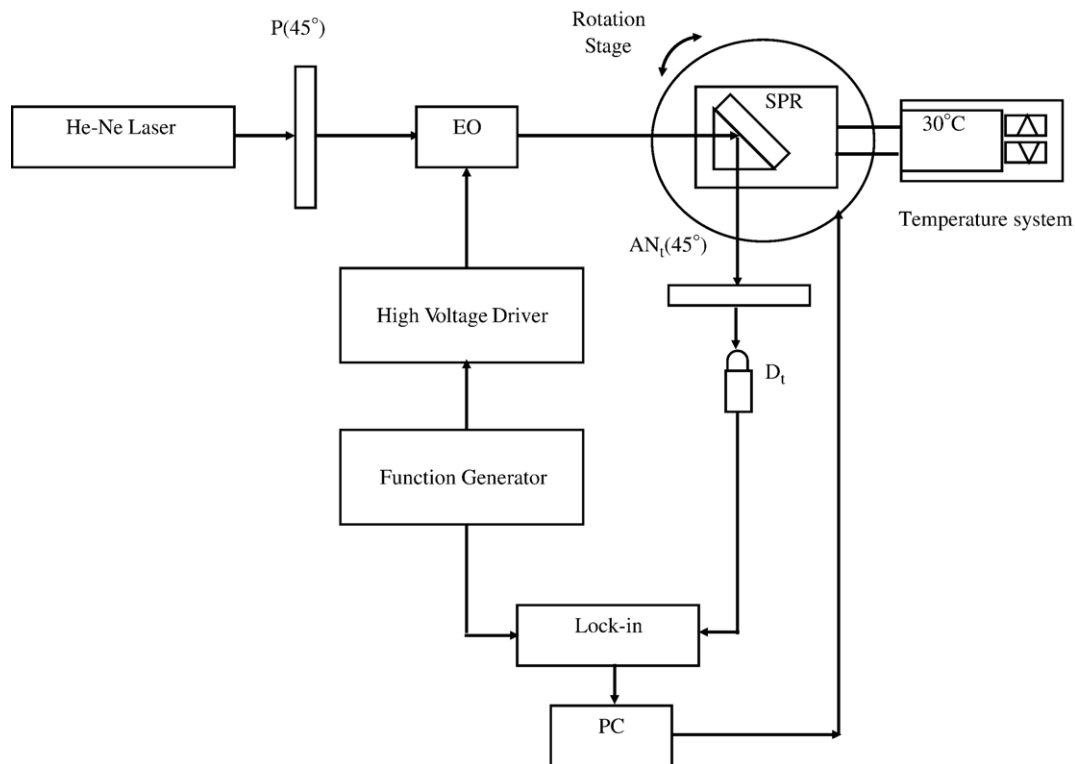


Fig. 2. Experimental setup.

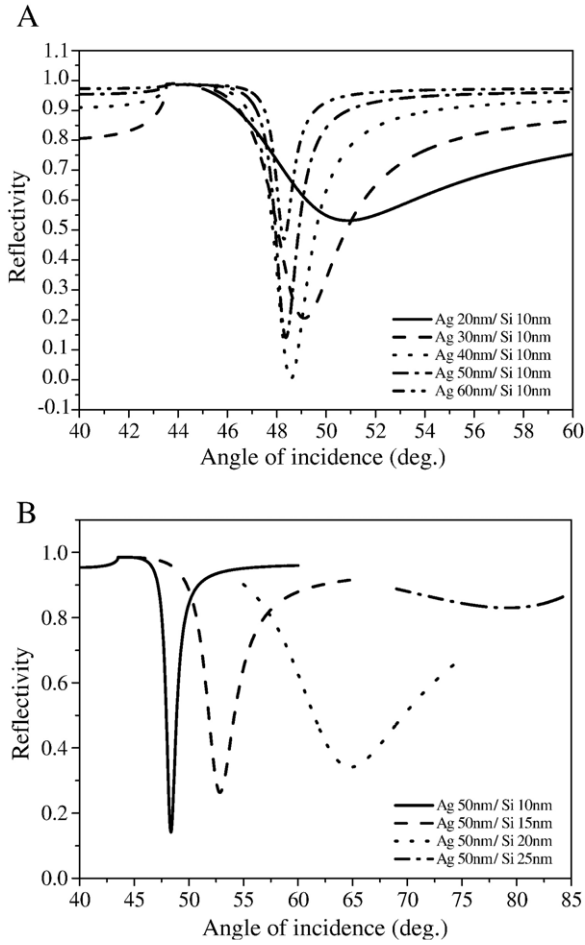


Fig. 3. Calculations of SPR reflectivity for a Ag/a-Si junction (A) for different thickness of the Ag film with the a-Si film thickness fixed at 10 nm and (B) for different thickness of a-Si film for a Ag film of 50 nm thick.

excite the SP at a metal–dielectric interface, $|r_s|=1$ and ϕ_s is almost a constant in Eqs. (1) and (2). We can therefore calculate $(\phi_p - \phi_s)$ and r_p from Eq. (2).

3. Theoretical simulation

In order to understand the experimental results, we have also developed a semi-empirical model for the temperature dependence of the SP excitation from a Ag/a-Si junction. For the metal (Ag), we have adopted a previously established temperature-dependent Drude model in which both the plasmon and collision frequencies vary with temperature: the former through a simple volumetric effect, and the latter through its dependence on the electron–phonon as well as electron–electron collisions, respectively [10]. Here we give a brief summary of the model in the following. Thus we have the metal dielectric function as follows:

$$\epsilon = 1 - \frac{\omega_p^2}{\omega(\omega + i\omega_c)}, \quad (3)$$

where ω_c is the collision frequency and ω_p the plasma frequency given by:

$$\omega_p = \sqrt{\frac{4\pi N e^2}{m^*}}, \quad (4)$$

with N and m^* the density and effective mass of the electrons, respectively. The collision frequency will have contributions from both phonon–electron and electron–electron scattering:

$$\omega_c = \omega_{cp} + \omega_{ce}. \quad (5)$$

As reported previously, for surface plasmon resonance (SPR), one must account for the temperature (T) variation of ω_p besides that for ω_c . Hence, as before, ω_p will depend on T via volumetric effects as follows:

$$\omega_p = \omega_{p0} [1 + \gamma(T - T_0)]^{-1/2}, \quad (6)$$

where γ is the expansion coefficient of the metal and T_0 is a reference temperature taken to be the room temperature. The collision frequency, ω_c , can then be modeled using the phonon–

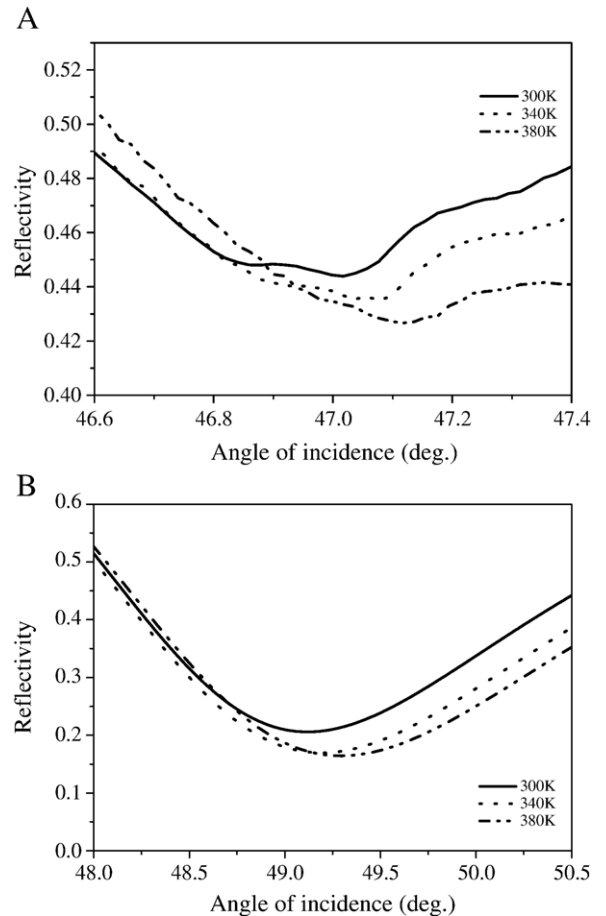


Fig. 4. Experimental (A) and theoretical (B) results for the temperature-dependent SPR reflectivity for the system in Fig. 1. Ag and a-Si film thickness are 30 nm and 10 nm, respectively; laser wavelength is 632.8 nm.

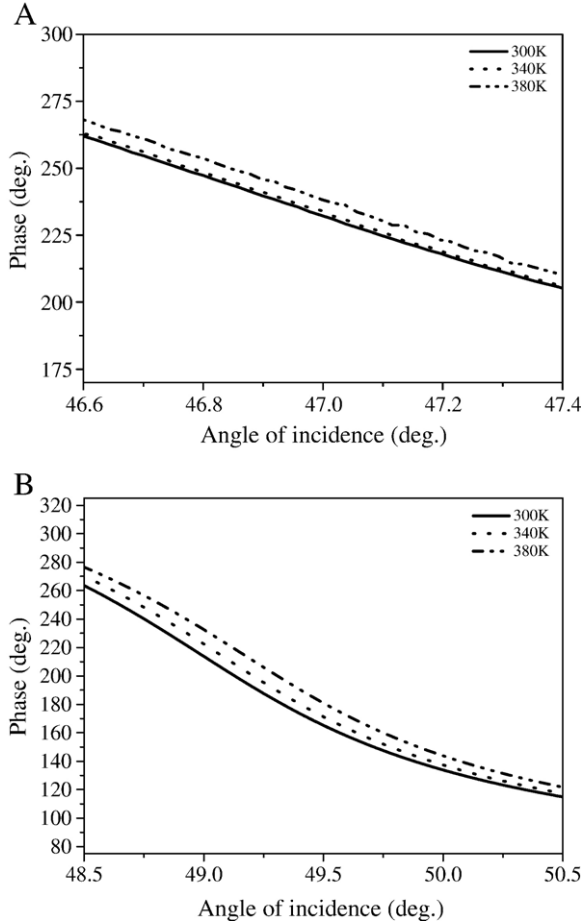


Fig. 5. Experimental (A) and theoretical (B) results for the temperature-dependent SPR phase measurements for the system in Fig. 1. Ag and a-Si film thickness are 30 nm and 10 nm, respectively; laser wavelength is 632.8 nm.

electron scattering model and the electron–electron scattering model, respectively. We thus obtain [11]:

$$\omega_{cp}(T) = \omega_0 \left[\frac{2}{5} + 4 \left(\frac{T}{\theta} \right)^5 \int_0^{\theta/T} \frac{z^4 dz}{e^z - 1} \right], \quad (7)$$

where θ is the Debye temperature and ω_0 is a constant to be determined from the static limit of the above expression together with the knowledge of the direct current conductivity. In addition, we have:

$$\omega_{ce}(T) = \frac{1}{12} \pi^3 \frac{\Gamma \Delta}{\hbar E_F} \left[(k_B T)^2 + (\hbar \omega / 2\pi)^2 \right], \quad (8)$$

where Γ and Δ are defined in Ref. [9].

For the semiconductor a-Si, we are not aware of any theoretical model for the temperature dependence of its optical constants, although one can retrieve the same information for bulk crystalline Si at certain wavelengths [12,13]. Because of this, we have decided to conduct separate measurements

using spectroscopic ellipsometry for the temperature dependence of these constants. The results for the two wavelengths in our experimental study can be numerically fitted as follows:

For the wavelength of 632.8 nm:

$$\begin{aligned} n(T) &= 3.08895 + 0.00119T - 1.14044 \times 10^{-5}T^2 \\ &\quad + 6.51458 \times 10^{-8}T^3 \\ k(T) &= 0.09386 + 0.00107T - 8.26437 \times 10^{-6}T^2 \\ &\quad + 1.58958 \times 10^{-8}T^3 \end{aligned} \quad (9)$$

For the wavelength of 1150 nm:

$$\begin{aligned} n(T) &= 3.55851 - 6.667116 \times 10^{-5}T - 1.69628 \times 10^{-6}T^2 \\ &\quad + 7.20826 \times 10^{-9}T^3 \\ k(T) &= 0.0901 + 1.25621 \times 10^{-4}T - 2.3746 \times 10^{-7}T^2 \\ &\quad - 3.34922 \times 10^{-10}T^3 \end{aligned} \quad (10)$$

With the above results in Eqs. (1)–(10), the SPR reflectance and phase as a function of temperatures can be calculated. Note

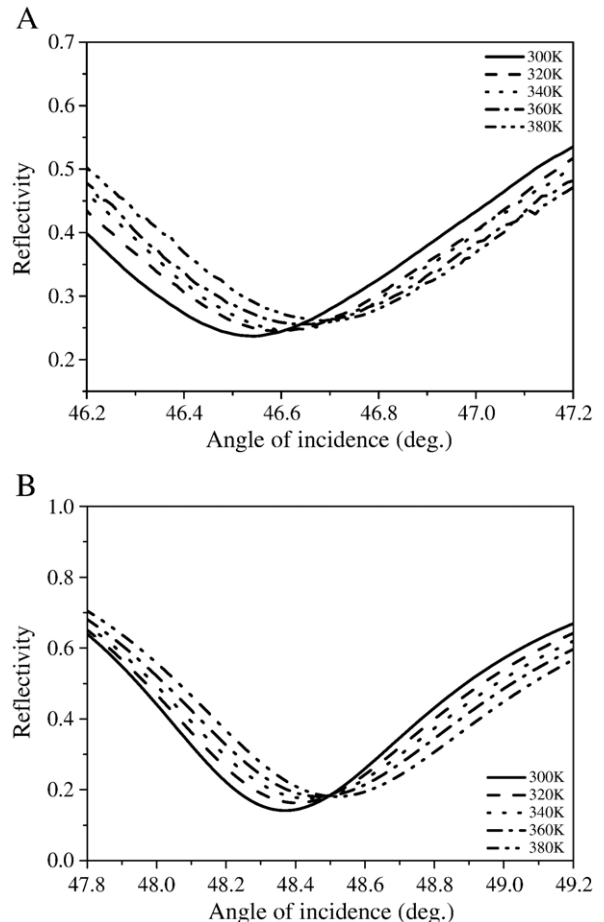


Fig. 6. Experimental (A) and theoretical (B) results for the temperature-dependent SPR reflectivity for the system in Fig. 1. The thickness of Ag film is 50 nm and the laser wavelength is 632.8 nm.

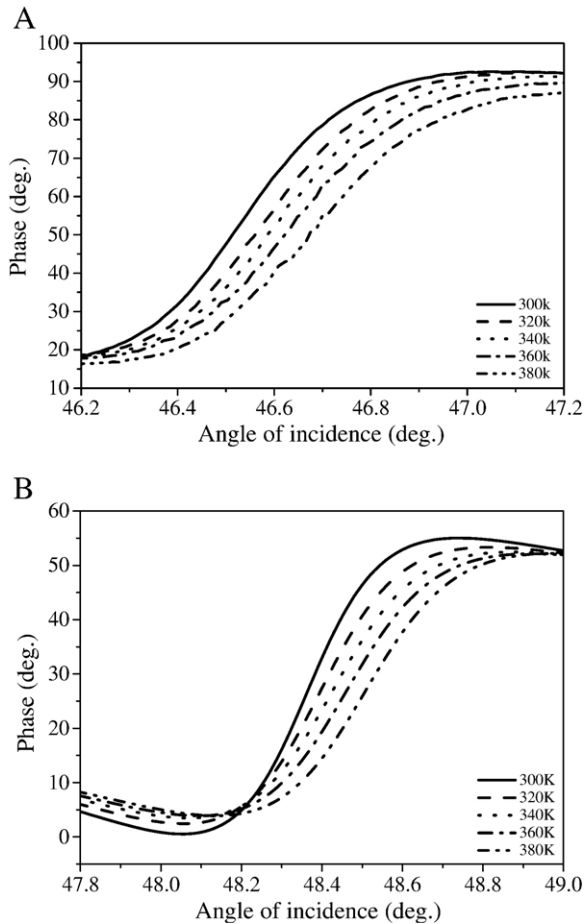


Fig. 7. Experimental (A) and theoretical (B) results for the temperature-dependent SPR phase measurements for the system in Fig. 1. The thickness of Ag film is 50 nm and the laser wavelength is 632.8 nm.

that we have also accounted for the expansion of the film thickness of the metal [11].

4. Results and discussion

We have performed both measurements and simulations on both the SPR reflectivity and phase change, over a temperature range of 300 K–380 K in steps of 20 K, for the configuration shown in Fig. 1 with different thickness for the metal film. For graphs turn out to be too clouded in the following figures, we shall report results only for three temperatures in this range. Just like the case with a pure metal film, there exists an optimal thickness of the metal film for the SP-driven MS junction to operate, as illustrated in Fig. 3A where a calculation of the SPR reflectivity for different metal thickness with a fixed a-Si thickness is performed. It is clear that the resonance width of the SPR curve becomes very narrow when the metal film attains its optimal value of thickness. The room temperature thickness of the a-Si film has been fixed at 10 nm throughout our study. Figs. 4–7 show the results for an incident wavelength of 632.8 nm, with Figs. 4 and 5 showing the reflectivity and phase results for a Ag film of room temperature thickness equal to

30 nm; while Figs. 6 and 7 showing the corresponding results for the case with a Ag-film thickness of 50 nm. Furthermore, we have also studied the effects at the longer wavelength of 1150 nm which is close to the room temperature band gap of a-Si. The corresponding results are shown in Figs. 8–11. From the results shown in the above figures, we make the following observations and comments:

- (1) As temperature increases, all the reflectivity curves become broadened due to the increase in damping of the metal. In addition, the resonance angles in both the reflectivity and phase plots shift to larger values at elevated temperatures. This can be understood from the dispersion relation for SP waves, together with the decrease in plasmon frequency and increase in collision frequency in the Drude model as the temperature increases [14].
- (2) From the phase plots, we see again the two possible patterns (from a sudden drop to a sudden rise across the resonance) as have been reported previously in the literature for a case with a pure metal film [15]. Note that the shift from one pattern to another depends on the competition of two damping rates in the plasmon of the metal, which in turn depends critically on the incident

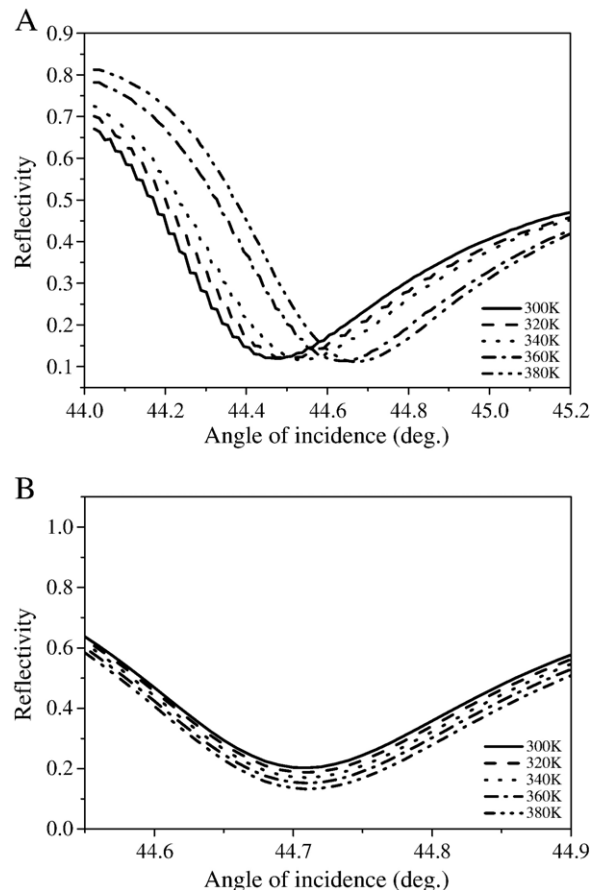


Fig. 8. Experimental (A) and theoretical (b) results for the temperature-dependent SPR reflectivity for the system in Fig. 1. Ag and a-Si film thickness are 30 nm and 10 nm, respectively; laser wavelength is 1150 nm.

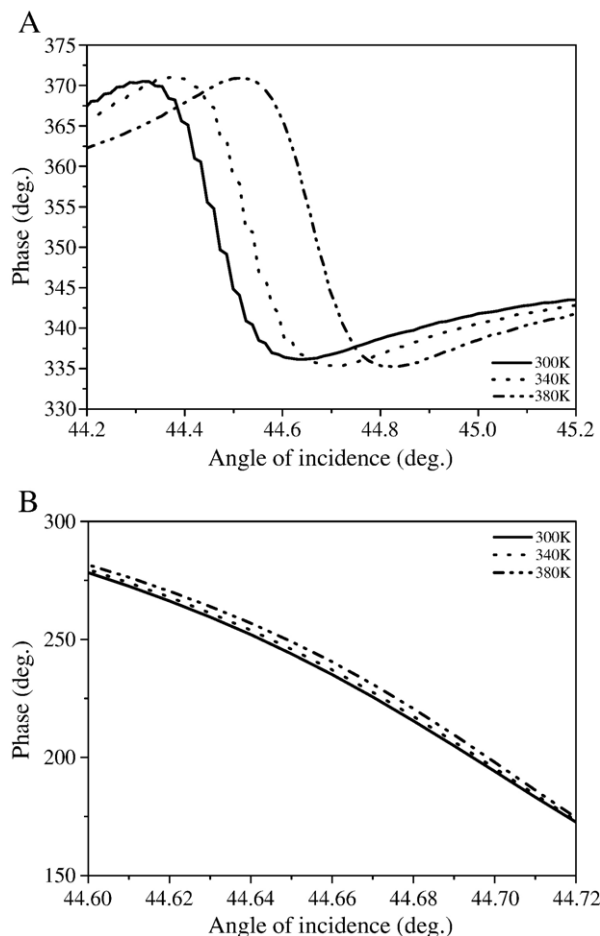


Fig. 9. Experimental (A) and theoretical (B) results for the temperature-dependent SPR phase measurements for the system in Fig. 1. Ag and a-Si film thickness are 30 nm and 10 nm, respectively; laser wavelength is 1150 nm.

wavelength and the thickness of the metal film [15]. In our MS junction, this critical thickness of the Ag film turns out to be about 40 nm. Thus we see, for both cases with 632.8 nm and 1150 nm incident wavelengths, the phase switches from a sudden drop as the angle increases (for the case with a 30 nm Ag film) to a sudden rise (for the case with a 50 nm Ag film). Data were also obtained for the case with a 40-nm film (not shown), analyzed in Table 1. Note that when the temperature is increased, the Ag-film expands which can lead to the switching of the phase curve from one pattern to another when the film thickness has expanded to cross the critical value.

- (3) The overall comparison between the simulation results and the experimental data is qualitatively reasonable, with all the behaviors of the experiment captured by the temperature-dependence model we introduce. Since the optical constants for a-Si used are fitted from ellipsometric measurements [see Eqs. (9) and (10) above], we conclude that the simple temperature-dependent Drude model we established previously [11] has some validity in the description of this SPR phenomenon. In particular, it is observed that agreement

between theory and experiment is much better for the 1150 nm case than that for the 632.8 nm case. This could be due to certain systematic error (e.g. oxide layer formation) in the ellipsometric measurement of the a-Si optical constants for the experiment in the latter case.

- (4) From the comparison between the results for 632.8 nm and those for 1150 nm, it is seen that the changes in the reflectivity, the resonance angle, and the phase are all more pronounced in the 1150 nm case than the corresponding changes in the 632.8 nm case. This is likely because 1150 nm (~ 1.08 eV photons) is close to the band-gap of a-Si, which leads to larger absorption by the a-Si thin film. Furthermore, this band-gap also decreases with a sensitive dependence on the temperature [16], which finally leads to a more pronounced temperature variation in the SPR data for the 1150 nm case.

We have further studied the sensitivities of various schemes in the SPR monitoring of temperature changes at the Ag/a-Si junction. By regarding our SPR-driven MS junction as a temperature sensor [5,6], one can analyze its sensitivity according to the monitoring of the resonance (dip) angle; the dip reflectance; and the resonance phase change as a function of

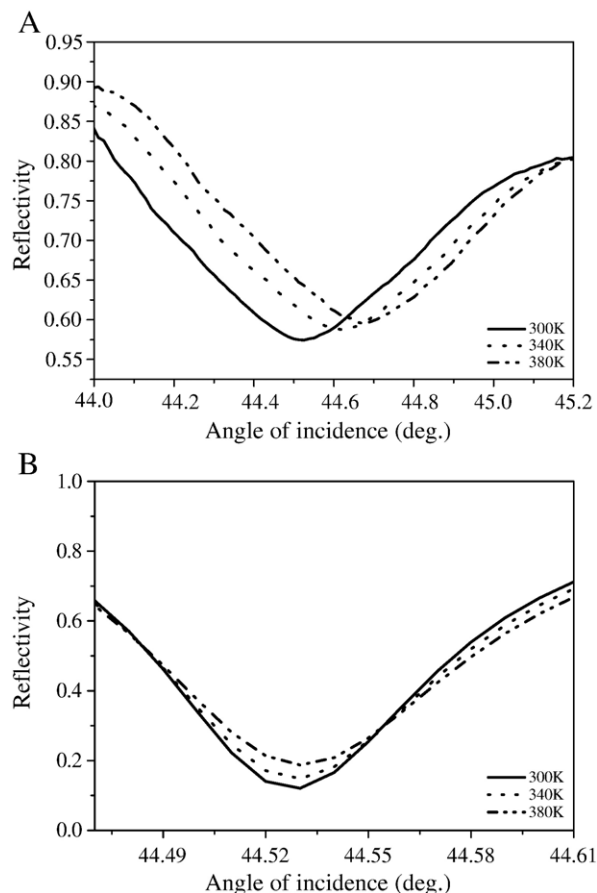


Fig. 10. Experimental (A) and theoretical (B) results for the temperature-dependent SPR reflectivity for the system in Fig. 1. The thickness of Ag film is 50 nm and the laser wavelength is 1150 nm.

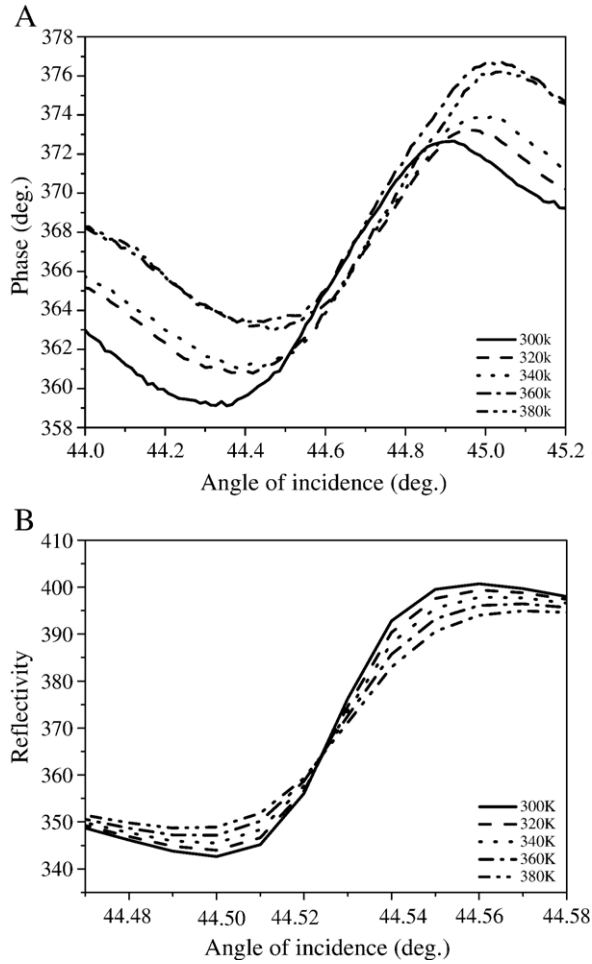


Fig. 11. Experimental (A) and theoretical (B) results for the temperature-dependent SPR phase measurements for the system in Fig. 1. The thickness of Ag film is 50 nm and the laser wavelength is 1150 nm.

temperature. By accounting for the limitations of our measuring apparatus with a minimum angular resolution (σ_θ) of 0.001° , a minimum reflectance resolution (σ_R) of 0.001, and a minimum phase resolution (σ_ϕ) of 0.01° ; we can compute the sensitivity of each monitoring scheme from plots of the resonance angle, resonance reflectance, and resonance phase change as functions of temperature. The “sensitivity factors” in the various schemes will be given by:

$$S_T^\theta = \frac{\Delta T}{\Delta \theta} \sigma_\theta, \quad S_T^R = \frac{\Delta T}{\Delta R} \sigma_R, \quad S_T^\phi = \frac{\Delta T}{\Delta \phi} \sigma_\phi, \quad (11)$$

where we have assumed a linear regression analysis over the relative small range of temperature change in our experiments. Results for the various sensitivity factors for the two wavelengths with different Ag-film thickness are summarized in Table 1. It is seen that a temperature sensor of high sensitivity (down to 0.037 K resolution) can be obtained using such a SPR-driven MS junction operated at a wavelength (1150 nm) close to the band-gap of the a-Si, and with the implementation of the

phase monitoring technique. Sensitivity down to a resolution of 0.168 K can be achieved using the same apparatus and incident wavelength (1150 nm) with the angle monitoring method. Compared to a conventional SPR temperature sensor using only a single metal film [14], a large improvement in sensitivity is achieved using a SPR-driven MS junction with angle interrogation technique; though the same improvement has not been achieved with the phase monitoring technique in our experiments. This seems to imply that the change in the refractive index of the a-Si over-layer will lead to more significant shift in resonance angle, and not as much in phase changes for the SPR curves at elevated temperatures. To further illustrate the difference between a “pure Ag” and a “Ag/a-Si” temperature sensor, we have in Fig. 12 shown explicit calculations for the SPR reflectivity and dip-angle of the two systems as functions of temperature, from which the unique role of a-Si can be clearly revealed. From Fig. 12B, it is observed that the rate of change of the dip angle per temperature rise is about 15% higher in the case when the a-Si film is present.

Moreover, although the changes in the reflectivity, the resonance angle, and the phase are more pronounced in the 1150 nm case than the corresponding changes in the 632.8 nm case, there is one exception. In the case of the Ag film thickness fixed at 40 nm, however, the sensitivity of phase measurements at 632.8 nm is 0.01 K, which is higher than that (~ 0.06 K) in the case of 1150 nm. As we have reported recently [17], the sensitivity of SPR sensor based on phase detection depends crucially on the incident wavelengths. There exists a “critical wavelength” across which two different phase change behaviors are observed [9,17]. A slight difference of incident wavelength could lead to drastically sensitivity change, if the incident wavelength is close to the critical wavelength. Though the value of this critical wavelength will change with the film thickness, however, optimal measurement can be achieved by controlling the incident wavelengths with fixed film thickness.

5. Discussions and conclusion

We have studied, both experimentally and theoretically, the temperature effects on a SPR-driven MS junction in terms of the resonance response of such a junction at elevated temperatures. Furthermore, if we assume that this SPR is correlated to the enhancement of the photocurrent for such a junction as established in some previous works [2,3], our results imply that such a SPR enhanced effect will in general decrease at high temperatures due to the increase of damping in the metal. However, we cannot conclude how the overall quantum efficiency of this junction will be affected with the increase in temperature, since our experiment was not set up for measurements of the photocurrents as a function of temperatures. While this problem has been studied previously for an ordinary Schottky junction [7,8], it has not been studied in the literature for such an SPR-driven junction. The situation will be more interesting in this latter case since while the increase in temperature will lower the SPR enhancement, it will also possibly lower the Schottky barrier of the junction in some devices [7,8]. Thus the two factors will compete to

Table 1

Comparison of the sensitivities among detection methods for (a) Ag 30 nm, (b) Ag 40 nm and (c) Ag 50 nm with wavelength at 632.8 nm and 1150 nm

(a) Ag 30 nm/Si 10 nm						
Modulation technique	Local slope		Instrument resolution		Calculated resolution (σ_T)	
Incident wavelength	632.8 nm	1150 nm	632.8 nm	1150 nm	632.8 nm	1150 nm
Angle	809	400	0.001	0.001	0.809 K	0.4 K
Reflectivity	2756	360	0.001	0.001	2.756 K	0.36 K
Phase	13.5	3.72	0.01	0.01	0.13 K	0.037 K
(b) Ag 40 nm/Si 10 nm						
Modulation technique	Local slope		Instrument resolution		Calculated resolution (σ_T)	
Incident wavelength	632.8 nm	1150 nm	632.8 nm	1150 nm	632.8 nm	1150 nm
Angle	678	168	0.001	0.001	0.678 K	0.168 K
Reflectivity	1111	650	0.001	0.001	1.111 K	0.650 K
Phase	1.036	6.10	0.01	0.01	0.01 K	0.061 K
(c) Ag 50 nm/Si 10 nm						
Modulation technique	Local slope		Instrument resolution		Calculated resolution (σ_T)	
incident wavelength	632.8 nm	1150 nm	632.8 nm	1150 nm	632.8 nm	1150 nm
Angle	503	505	0.001	0.001	0.503 K	0.505 K
Reflectivity	822	822	0.001	0.001	0.822 K	0.822 K
Phase	44.492	19.02	0.01	0.01	0.44 K	0.190 K

The thickness of a-Si is fixed at 10 nm.

determine the overall change in quantum efficiency of such a junction at elevated temperatures. Future experiments in this direction will be of interest.

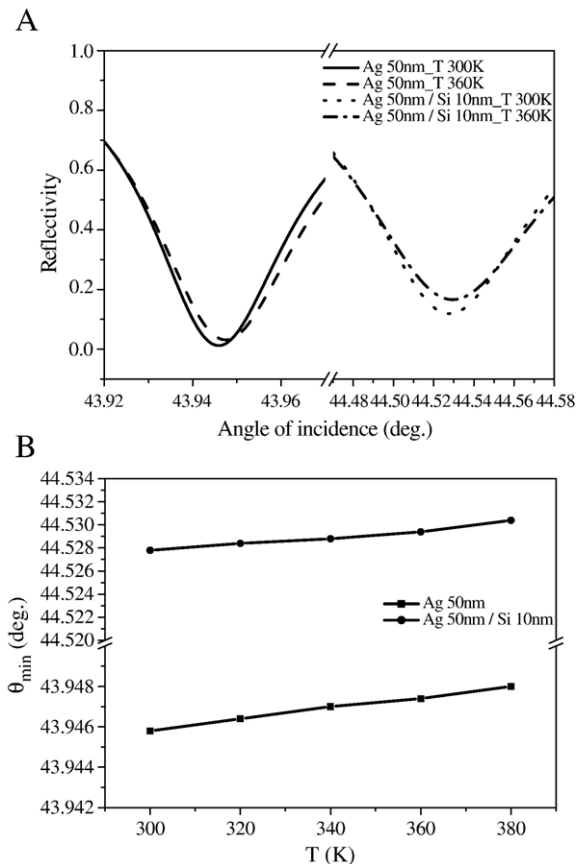


Fig. 12. Calculations of (A) SPR reflectivity and (B) dip-angle for both pure Ag and Ag/a-Si systems as a function of temperature.

We have also explored the application of our junction as a temperature sensor, and have come to the conclusion that very sensitive temperature monitoring can be achieved by operating the device at 1150 nm which is close to the band-gap of the silicon. It also re-confirmed what is already established in the literature that phase monitoring is by far the most sensitive way to detect any changes in an SPR experiment. In addition, the simple temperature dependence model we introduced seems to be able to capture most of the qualitative behaviors observed in all the experiments.

Acknowledgments

H.P. Chiang acknowledges financial support from Center of Nanostorage Research, National Taiwan University, under grant number MOEA #95-EC-17-A-08-S1-0006 and the National Science Council of ROC under grant numbers NSC 95-2112-M-019-002 and NSC 95-2120-M-019-001, and Center for Marine Bioscience and Biotechnology, National Taiwan Ocean University with grant numbers NTOU-AF94-05-04-01-01 and NTOU-AF94-05-04-01-02., EJS acknowledges research funding from NSF IDBR(0500812), and PTL acknowledges the support of a research grant from Intel Corporation.

References

- [1] See, e.g., S.M. Sze, K.K. Ng, *Physics of Semiconductor Devices*, Wiley, New York, 2006.
- [2] M.J. Cazeca, C.C. Chang, A.S. Karakashian, *J. Appl. Phys.* 66 (1989) 3386.
- [3] C. Daboo, M.J. Baird, H.P. Hughes, N. Apsley, M.T. Emeny, *Thin Solid Films* 201 (1991) 9.
- [4] H. Raether, *Surface Plasmons on Smooth and Rough Surface and on Gratings*, Springer, Berlin, 1988.
- [5] P.I. Nikitin, A.A. Beloglazov, *Sens. Actuators, A, Phys.* 41–42 (1994) 547.
- [6] S.K. Özdemir, G. Turhan-Sayan, *J. Lightwave Technol.* 21 (2003) 805.
- [7] J.H. Werner, H.H. Guttler, *J. Appl. Phys.* 73 (1993) 1315.

- [8] J. Osvald, J. Kuzmik, G. Konstantinidis, P. Lobotka, A. Georgakilas, *Microelectron. Eng.* 81 (2005) 181.
- [9] A similar setup was also presented in, H.-P. Chiang, J.-L. Lin, R. Chang, S.-Y. Su, P.T. Leung, *Opt. Lett.* 30 (2005) 2727.
- [10] H.-P. Chiang, Y.C. Wang, P.T. Leung, *Thin Solid Films* 425 (2003) 135.
- [11] See also, H.-P. Chiang, P.T. Leung, W.S. Tse, *Solid State Commun.* 101 (1997) 45.
- [12] G.E. Jellison Jr., D.H. Lowndes, *Appl. Phys. Lett.* 41 (1982) 594.
- [13] G.E. Jellison Jr., H.H. Burke, *J. Appl. Phys.* 60 (1986) 841.
- [14] H.-P. Chiang, Y.-C. Wang, P.T. Leung, W.S. Tse, *Opt. Commun.* 188 (2001) 283.
- [15] H.-P. Chiang, H.-T. Yeh, C.-M. Chen, J.-C. Wu, S.-Y. Su, R. Chang, Y.-J. Wu, D.P. Tsai, S.U. Jen, P.T. Leung, *Opt. Commun.* 241 (2004) 409.
- [16] N. Do, L. Klees, P.T. Leung, F. Tong, W.P. Leung, A.C. Tam, *Appl. Phys. Lett.* 60 (1992) 2186.
- [17] H.-P. Chiang, J.-L. Lin, Z.-W. Chen, *Appl. Phys. Lett.* 88 (2006) 141105.